

Examining the Impact of Using Hemispherical Dimples-protrusions on Heat Transfer and Pressure Drop in the Finned-tube Heat Exchanger with Different Configurations

O. Baharlouei and S. Talebi[†]

Department of Mechanical Engineering, Yazd University, Yazd, Iran

[†]Corresponding Author Email: talebi_s@yazd.ac.ir

ABSTRACT

In comparison to a plain fin, the addition of dimples or protrusions to the fins of a finned tube heat exchanger significantly affects the promotion of heat transfer. The impact of the number of dimples or protrusions and the arrangement of inline and staggered configurations on pressure drop and heat transfer is examined numerically in this research. The outcomes demonstrate that increasing the number of dimples and protrusions significantly affects heat transfer magnitude and pressure drop. Increasing the number of dimples and protrusions within the Reynolds number range of 150-1200 enhances the friction coefficient and heat transfer by 108%-163% and 16%-112%, respectively, in contrast to the plain fin. In evaluating the result of the arrangement of inline and staggered configurations, the heat transfer amounts of these two models are almost the same, and the friction coefficient is higher in the model that uses the arrangement of inline. In the inline arrangement model utilizing dimples-protrusions, the resultant heat transfer and friction coefficient increase 11%-92% and 64%-113% within the Reynolds number range of 150-1200, respectively, compared to the plain fin.

Article History

*Received October 18, 2024
Revised January 19, 2025
Accepted February 16, 2025
Available online May 5, 2025*

Keywords:

*Nusselt number
Reynolds number
Dimple
Fin
Finned tube heat exchanger
Staggered arrangement
Inline arrangement*

1. INTRODUCTION

Finned tube heat exchangers have extensive usage in various industries where heat transfer is a vital aspect. The finned tube heat exchanger has manifold applications, encompassing air cooling, intercooler of diesel engines, oil cooling, waste heat recovery, dryers, air heaters, steam condensers, and generator coolers. Typically, air is employed to cool or heat fluids like air, water, oil, or gas in this sort of heat exchanger. The finned tube heat exchanger is preferred when the heat transfer coefficient of one fluid (air) is inferior to that of another fluid (liquid). In this sort of heat exchanger, the fluid with the superior heat transfer coefficient traverses the tube, while the fluid having a lesser heat transfer coefficient flows outside the tube. The flow over tubes (air side) exhibits the highest thermal resistance, emphasizing the importance of enhancing heat transfer on this side. A feasible approach to improving finned tube heat exchanger performance is through increasing fin area. Utilization of dimpled fins provides the possibility of heat transfer enhancement without exacerbating the pressure drop.

Azad et al. (2000) examined an experimental investigation of heat transfer using dimples on surfaces compared to plain surfaces. The study comprised two cases, each with a distinct quantity of dimples. The dimples' diameter was 0.635 cm alongside their depth of 0.3175 cm. In the model of the dimpled surfaces, The Nusselt number was nearly equivalent to the other model with plain surface. However, the increase in surface area due to dimples resulted in higher total heat transfer. The heat transfer rate resulted in 33.8% and 9% higher than the plain surface for maximum and minimum numbers of dimples, respectively. Cheraghi et al. (2020) researched a numerical investigation into the enhancement of heat transfer and pressure drop in a heat exchanger using the dimpled tube. The research was carried out in 27 cases of tube diameters measuring 9 mm, 13 mm, 5 mm, and 18 mm, with varying depths and pitches for the dimples. In the 25th case, which featured dimples with the largest diameter, depth, and smallest pitch, the friction coefficient and the Nusselt number in the dimpled tube were 44 and 6 times more than in a plain tube surface, respectively.

Du et al. (2020) investigated numerical research on heat transfer variations in gas turbine blade cooling

Nomenclature			
C_p	specific heat of the fluid	Pr	Prandtl number
D	tube diameter fin collar outside diameter	p	local pressure
F_p	fin pitch	p_{in}	inlet pressure
F_t	thickness	Q	heat transfer rate
f	friction factor	Re	Reynolds number based on fins spacing
H	fins spacing	T_{in}	inlet temperature
j	Colburn factor	T_w	wall temperature
h	average heat transfer coefficient	T_{out}	outlet temperature
$\frac{j}{f}$	flow area goodness factor	ΔT	log mean temperature difference
k_f	thermal conductivity of fin	u_{in}	inlet velocity
k	fluid thermal conductivity	\vec{V}	velocity vector
L	fin length	Greek symbols	
n	number of rows of tubes	μ	dynamic viscosity
Nu	Nusselt number	ρ	density
P_t	transverse tube pitch		
P_l	longitudinal tube pitch		

applications through the use of dimples affixed at various positions on the pin-finned channel. These dimples were partially spherical; the depth-to-diameter ratio was 0.2. The findings demonstrated that the placement of the dimples greatly influenced heat transfer and the flow structure. Specifically, when dimples were located in the area of wake, the Nusselt number experienced only a modest increase of 3.52% in comparison to the channel without dimples. Additionally, the friction coefficient increased by 1.82%. This low enhancement in the Nusselt number was attributable to the occurrence of wake and reversed flow. Furthermore, in instances where the dimples were situated amidst a pair of pin fins, a noteworthy rise of 20.94% resulted in the Nusselt number, and the friction coefficient experienced a decline of 1.69% in contrast to the pin-finned channel without dimples.

Fan et al. (2012) conducted a numerical analysis of ellipse-shaped dimples for a finned-tube heat exchanger. The study was conducted with a staggered arrangement, using a diameter of 9.52 mm for tubes and two tube rows. The researchers concluded that the heat exchanger with dimples demonstrated a higher value of Nusselt number and friction coefficient than the plain fin. Moreover, the heat transfer rate increased by 13.8%-30.3% in the finned-tube heat exchanger with dimples compared to the plain fin.

Gupta et al. (2019) researched an experimental investigation into the increase of heat transfer in heat sink-plain fin by introducing dimples and protrusions with the arrangement of inline and staggered configurations. In the dimpled fin, the Nusselt number and friction coefficient exhibited higher values relative to the other model without using dimples. Moreover, flow performance and the fin's heat transfer were notably reliant on the dimple's depth, and an increase in depth led to a boost in heat transfer. The optimal heat sink performance with dimpled fins was contingent upon the depth-to-diameter ratio of the dimple, which was 0.5, and the longitudinal pitch-to-diameter ratio of the dimple, which was 2.5. Katkhaw et al. (2014) studied experimental research on heat transfer increase through the incorporation of elliptical dimples with a depth of 12 mm in ten distinct models on a plain surface.

Results indicated that in the configuration of staggered dimples, the highest coefficient of heat transfer value was 15.8% greater than that of the other model that was without dimples. Additionally, in the inline arrangement of dimples, the largest Nusselt number value was 21.7% higher than that of the surface without dimples.

Kumar et al. (2017) studied experimental and numerical research on enhancing heat transfer by integrating dimples with a depth-to-diameter ratio of 1 into the tube of a heat exchanger. The study examined different scenarios that varied the stream-wise and span-wise spacing of the dimples. Based on their findings, a 15-spacing case for stream-wise and span-wise arrangements increased the heat transfer and thermal-hydraulic efficiency by 3.18 and 2.87 times greater, respectively, compared to a plain tube. This indicated that the inclusion of dimpled tubes was a promising technique for enhancing heat transfer in heat exchangers. Li et al. (2016) researched an experimental and numerical investigation into the effects of dimples on a tube heat exchanger. The surface of a tube, which had a diameter of 17.272 mm, displayed a pattern of dimples that were arranged in a staggered configuration and had a diameter of 5 mm. The dimples led to an increase in turbulence levels through boundary layer mixing and secondary flow generation. Additionally, the Nusselt number and the friction coefficient exhibited higher values in dimpled tubes than in plain tubes.

Luo et al. (2016) conducted an experimental investigation to examine the friction coefficient and the heat transfer performance in pin fin ducts with various dimple arrangements in the context of the blade of gas turbine cooling. This study was conducted using three-pin fin and dimple arrangement models at a depth to dimple diameter ratio of 0.2. The findings indicated that dimples could significantly increase endwall heat transfer, particularly when positioned in an inline pattern with pin fins. This arrangement was also associated with a low friction coefficient.

Piper et al. (2019) conducted a numerical investigation aimed at enhancing the heat transfer of the

pillow-plate heat exchanger. It was approachable by introducing a staggered arrangement of dimples, each with a radius of 4.2 mm, onto the surface. The results revealed a notable increase of 2.2% in the heat transfer coefficient, along with an 8.7% decrease in pressure drop, compared to the plain surface. Furthermore, an overall improvement of 11.2% in the efficiency of thermo-hydraulic resulted. Rao et al. (2012a) conducted an experimental study concerning pressure drop and heat transfer in pin fin-dimple channels of varying dimple depths. The study was conducted under a range of conditions including depth to diameter of dimple ratios of 0.1, 0.2, and 0.3. The outcomes showed that adding dimples in the pin fin channel led to a 19% improvement in the performance of heat transfer. Furthermore, the Nusselt number improved with an enhancement in dimple depth. The pressure drop was also related to dimple depth, as decreasing the depth of the dimple led to a 17.6% decrease in the friction coefficient. Rao et al. (2015) performed experimental and numerical investigations on the heat transfer of surfaces using teardrop and spherical dimples, each with a diameter of 20 mm and staggered arrangement through experimental and numerical methods. The findings were subsequently compared with those obtained from plain surfaces. Results revealed that the utilization of dimples in channels yielded an average heat transfer and friction coefficient that were 1.5-1.7 times and 1.2-2 times more than that of the plain channel, respectively.

Seo et al. (2012) conducted a comprehensive investigation using numerical and experimental processes to explore the heat transfer performance of dimpled tubes in cooling applications. Specifically, they employed a spiral cooling model that incorporated 22 tubes with plain surfaces, as well as dimpled tube models with four and ten rectangular tubes measuring 26.5 mm x 150 mm. The outcomes of their study demonstrated that the dimpled tube heat exchanger outperformed its plain-surfaced counterpart, with the dimpled tube model featuring ten tubes exhibiting the highest heat transfer performance. Vorayos et al. (2016) studied an experiment to examine the heat transfer process using spherical dimples affixed to a plain surface. Fourteen different models were analyzed, with the dimples possessing a diameter and depth of 30 mm and 9 mm, respectively. The dimpled surface was arranged in both staggered and inline configurations. The outcomes of this experiment revealed that the Nusselt number was 26% and 25% higher for the staggered and inline structures, respectively, in contrast to the plain surface.

Vignesh et al. (2017) investigated numerical and experimental examinations aimed at exploring heat transfer performance in tube heat exchangers equipped with spherical dimples. The outcomes of their investigation indicated that the existence of dimples considerably increased the heat transfer, effectiveness, and total heat transfer coefficient when evaluated to heat exchangers containing plain tube surfaces. Wu et al. (2014) conducted a numerical investigation about the impact of the quantity of tube rows and dimples on the fin in the context of finned-tube heat exchangers. The study was carried out with 2, 3, 4, and 5 tubes of external diameter 10 mm, arranged in a staggered manner. The

results revealed that dimpled fins exhibited higher friction coefficients and Nusselt numbers compared to plain fins. Furthermore, an enhancement in the quantity of tube rows led to a reduction in the Nusselt number. The two-row tube configuration was identified as offering superior performance for the heat exchanger, outperforming the other models.

Wang et al. (2016) researched a comprehensive experimental and numerical investigation on the impact of dimples in enhancing heat transfer within a thermoelectric generator's heat exchanger. This study focused on analyzing pressure drop and heat transfer for a dimple depth-to-diameter proportion of 0.2. Ultimately, they achieved optimal performance of heat transfer while minimizing pressure drop with this generator. Additionally, they determined that utilizing a dimpled surface at a Reynolds number equal to 25000 resulted in a 15% increase in production power compared to without using dimples.

Wang et al. (2018) researched an experimental and numerical investigation to assess the efficacy of a thermoelectric generator for automobiles. The study involved a comparison of two types of heat exchangers: one fitted with fins inserted into the surface and the other with a dimpled surface, featuring a depth and diameter of 4.5 mm and 16 mm, respectively. The researchers determined that replacing the fins with the dimpled surface led to a slight increase in temperature difference and output power, owing to the increased heat transfer of the dimpled surface. Additionally, the thermoelectric generator featuring a dimpled surface experienced a 20.57% reduction in pressure drop. The net automotive thermo-electric generator's power and performance were 173.6% and 172% higher, respectively, when using the dimpled surface.

Zheng et al. (2018) performed an experimental study of the effectiveness of heat transfer in a tube-fin heat exchanger employing four distinct fin models. Notably, the dimpled fin model, possessing 6 and 9 dimples, and featuring eight tube rows at varying Reynolds numbers, exhibited a higher friction coefficient and Nusselt number relative to the plain fin. Lotfi and Sunden. (2019) conducted numerical research on the impact of utilizing various types of dimples in finned tube heat exchangers, such as ED, CFD, TPD, LwTD, and UwTD. The findings indicated that all of the models incorporating dimples on fins exhibited higher Nusselt numbers and friction factors compared to plain fins in different Reynolds numbers. Furthermore, the LwTD model demonstrated the most significant increase of heat transfer.

Jing et al. (2019) carried out the augmentation of heat transfer through the utilization of dimples-protrusions situated on the trailing edge of the gas turbine blade for cooling performance. The researchers determined the utilization of dimples-protrusions demonstrated higher friction factor and Nusselt number values in contrast to smooth blades in different Reynolds numbers. Aroonrat and Wongwises (2019) investigated experimental research about the heat transfer and pressure drop in the process of condensation of R-134a flowing within dimpled tubes with dimples of depths measuring 0.5, 0.75, and 1 mm.

The findings demonstrated that the utilization of these dimpled tubes exhibited a noteworthy augmentation in heat transfer and pressure drop. Using dimpled with the most depth produced the highest increase in heat transfer and penalty in pressure drop, with values up to 83% and 892% more elevated than those observed in the smooth tubes, respectively.

Ying et al. (2021) studied numerical and experimental analysis to examine the impact of utilizing hemispherical and rhombus dimples on heat transfer in dimples of varying depths. They observed that the Nusselt number in the shape of a hemispherical dimpled channel increased proportionally with the Reynolds number. The results demonstrated that the improvement of the Nusselt number in channels with a higher diameter-depth ratio was greater than in other models. Additionally, in hemispherical dimple channels, characterized by three different radius-depth proportions, the heat transfer coefficient was approximately 27.2% more than that of the rhombus dimple channel.

Bi et al. (2013) executed a numerical investigation focused on implementing dimples and cylindrical grooves to enhance the cooling heat transfer mechanisms within mini-channels. Their findings indicated that incorporating dimples yields the most significant enhancement in the performance of heat transfer. Xie et al. (2018) examined a computational analysis of the utilization of dimples and protrusions within a tube. They assessed the impact of the depth, pitch, and radius of protrusions on the heat transfer performance. The researchers determined that the efficacy of heat transfer is significantly enhanced through the implementation of dimpled and protruded surfaces; furthermore, they concluded that the Nusselt number and the friction coefficient exhibit an enhancement in correlation with the augmentation of the protrusion depth. Rao et al. (2012b) undertook a comprehensive numerical and experimental investigation concerning heat transfer mechanisms in channels characterized by pin fin-dimple configurations and pin fin arrangements. Their findings indicated that the heat transfer performance of the pin fin-dimple configuration surpasses that of the other model by 8%.

Sangtarash and Shokuhmand. (2015) executed a numerical and experimental investigation into the influence of incorporating dimples and perforated dimples on multi-louvered fins arranged in inline and staggered configurations. The study concluded that the introduction of a dimple on the louver surface results in an enhancement of the j coefficients and friction coefficients. Furthermore, the heat transfer efficacy was superior in staggered arrangements. Hwang et al. (2012) executed a numerical investigation to augment heat transfer performance within tube-fin heat exchangers incorporating delta winglet vortex generators, subsequently comparing the findings with a model employing plain fins. The researchers deduced that the fin integrated with delta winglet vortex generators demonstrated a reduction in pressure loss in contrast to a heat exchanger with plain fin, while also noting an enhancement in heat transfer performance at elevated air velocities. Malapur et al. (2022) performed a numerical

investigation on the enhancement of heat transfer in a pipe heat exchanger with internal and external dimples. They discovered that the pressure loss for cold as well as hot fluids enhanced when dimples were added to the pipe surfaces. The boundary layer is disturbed when the hot fluid passes through the pipe and comes into contact with a dimple; the same is true for the cold fluid that passes over a dimple on the pipe's exterior. In dimpled tube heat exchangers, which have dimples inside and outside the pipe, this disruption greatly increases the heat transfer coefficient between the hot and cold fluids. Under similar input and boundary circumstances, it was discovered that the total heat transfer coefficient of internally and externally dimpled helical counter heat exchangers was higher compared to that of smooth counter heat exchangers.

Kaood et al. (2022) studied numerical research on the thermal-hydraulic conical tube performance with dimples. In comparison to conventional smooth geometrical arrangements, the results revealed significant increases in heat transfer and overall thermal-hydraulic performance. The converging tube with dimples (diameter ratio = 1.5) achieved the highest Performance Evaluation Criteria (PEC) value, indicating a 29.54% enhancement over the smooth geometry with a diameter ratio of 1. The average PEC values across the entire range of Reynolds numbers showed an 8.03% enhancement in contrast to the smooth geometry featuring a diameter ratio of 1 for all cases examined. Furthermore, the convergent tube with dimples (diameter ratio = 1.5) exhibited the maximum increase in the Nusselt number ratio, reaching 2.72 at Re of 3000, which corresponds to a 121.4% enhancement compared to the smooth configuration. Elsaid et al. (2023) conducted an experimental study to enhance the performance of cool water air conditioning cooling coils with various dimple fin geometries. They found that the heat exchanger featuring a curved-sided triangular fin dimple configuration exhibited a superior flow area goodness factor and Nusselt number. Specifically, the cooling coil heat exchanger with 170 fins achieved a Nusselt number that was 94.4% higher than that of the heat exchangers with 140 fins and approximately 27.3% greater than that of the heat exchangers with 155 fins. Furthermore, the efficiency proportion of energy for the cooling coil with 170 fins surpassed that of the coils with 140 and 155 fins by approximately 24.68% and 12.94%, respectively. Mehrjardi et al. (2023) carried out a numerical analysis of the impact of elliptical dimples on the performance of heat transfer in shell and tube heat exchangers. They found a 40.6% enhancement in the heat capacity of these heat exchangers. By enhancing heat capacity through modified surfaces like dimples, the dimensions and weight of this type of heat exchanger can be significantly reduced, benefiting industrial applications.

Paul et al. (2023) conducted a numerical study on the performance of heat exchangers, focusing on enhancements achieved by incorporating spherical dimples on the fin surfaces. They experimented with variations in dimple depth, position, and quantity. The configuration featuring 26 dimples on each side of the fin at a depth of 5.5 mm exhibited the greatest increase in the

Nusselt number, with a 7.33% improvement over a smooth fin. Among all configurations, the optimal case was identified as having 32 dimples on both sides of the fin at a depth of 3 mm, which resulted in a 5.71% increase in the Nusselt number and a 6.75% higher friction factor compared to the smooth fin. Furthermore, both configurations with 32 and 26 dimples at a depth of 5.5 mm achieved the highest temperature effectiveness of 11.45%, while the smooth fin only reached a value of 10.16%. Song et al. (2024) performed a numerical study to improve the performance of a circular tube-fin heat exchanger by incorporating ellipsoidal dimples and protrusions at five different attack angles. They discovered that the Nusselt number (Nu) increased by as much as 29.01%, and the thermal performance factor improved by 16.1% compared to a smooth channel. The use of ellipsoidal dimples and protrusions significantly enhances heat transfer on the fin side of circular tube-fin heat exchangers.

Luo et al. (2024) executed a numerical study to enhance the power output of a thermocouple generator by incorporating dimples on the fin. Their findings indicate that increasing the quantity of dimple columns and the radius of the dimples enhances the heat exchanger's potential to transfer heat, although this also results in an increase in back pressure loss for the exhaust flow. Through optimization, they determined that the optimal dimple configuration consists of 8 columns with a radius of 1.45 mm, resulting in the highest net power production of 62.46 W. The performance of the improved automobile thermoelectric generator with dimpled fins significantly outperforms that of traditional plate-fin structures, with improvements in conversion efficiency, power generated, voltage of output, and net energy generation of 16.07%, 28.95%, 13.56%, and 10.09%, respectively. Sen et al. (2024) conducted a numerical study on enhancing heat transfer in fins using dimples and protrusions. The total heat transfer efficacy of dimpled and protruded fins increases with depth. Initially, performance rose with increasing hole diameter but eventually declined; conversely, it first decreased and then improved with an enhancement offset. The protruded and dimpled fins achieved the highest increase factor with a diameter of 3.4 mm. Additionally, the performance evaluation criteria (PEC) for the new fin showed an increase of 23.7% in contrast to the porous fin.

Multiple investigations have been analyzed on the impact of dimples; however, research on the influence of dimples-protrusions arrangement and quantity in the implementation of finned-tube heat exchangers is restricted. Consequently, the focal point of this research is to investigate a three-dimensional (3D) numerical investigation on the impact of staggered and inline arrangements of dimples-protrusions, along with the impact of their quantity on heat transfer and pressure drop in the utilization of finned-tube heat exchangers.

2. GEOMETRY

Figure 1 illustrates the physical model of a finned-tube heat exchanger. The computational domain utilized for the simulation encompasses two half-fins situated at

the upper and lower boundaries, as well as the entire fluid area that exists between these two half-fins. In consideration of the fin's thin thickness, a protrusion is constructed on the upper surface through the fabrication of a dimple on the lower surface of the fin. In this investigation, the computational domain A is utilized to examine the effect of dimples-protrusions arrangement and quantity on a spherical shape with a diameter of 4.8 mm.

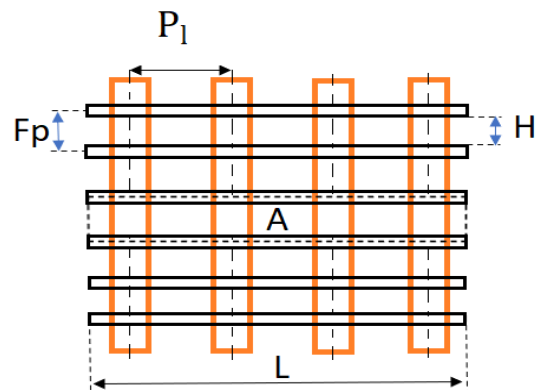


Fig. 1 Simulated heat exchanger

Three distinct models are employed. The first two models consist of 12 dimples which are arranged in an inline and staggered configuration as model (a) and model (b), respectively. The third model features 24 dimples in an inline arrangement for model (c). The computational region and boundary conditions are indicated in Fig 2. Specifically, the inlet extends to nearly one times the fin's length, while the outlet extends approximately four times the length of the fin to avoid any adverse effects on the computational domain and to make sure the absence of reverse flow at the outlet boundary. Table 1 indicates the specifications and dimensions of the computing domain.

3. GOVERNING EQUATIONS AND NUMERICAL MODEL

Assumptions are made in the present study, namely that the air-fluid is Newtonian, and the flow is incompressible and three-dimensional. Citing reference of Fan et al. (2012), which pertains to the utilization of dimples in finned-tube heat exchangers, it is determined that the numerical solution is derived for laminar flow. Moreover, due to the low Reynolds number, it is appropriate to assume that the flow is laminar. As the flow variables, including pressure, velocity, and temperature, are unchanging at a particular point in time, the numerical solution is conducted as a steady flow.

The boundary conditions are:

1. The condition of non-slip on all solid surfaces.
2. Constant temperature of 353K on the surface of the tubes.
3. Specific velocity and temperature at the inlet boundary, the temperature is 293K, and the velocity according to the Reynolds number is between 0.8528 m/s and 6.823 m/s.

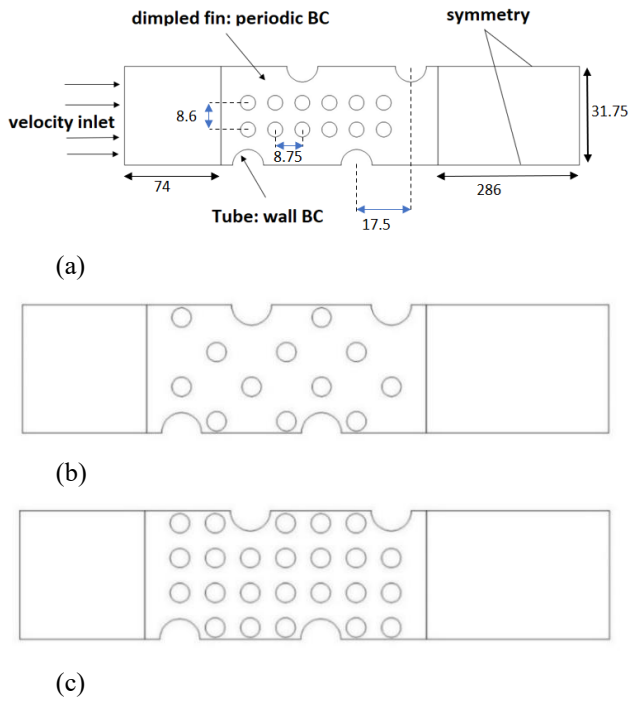


Fig. 2 Model (a) in-line arrangement of dimples-protrusions, model (b) staggered arrangement and model (c) is the investigation of the effect of the number of dimples-protrusions in in-line arrangement

Table 1 Geometric parameters of heat exchanger

Parameters	Values
Fin and tube arrangement	Staggered
Number of rows of tubes, n	4
Tube diameter fin collar outside diameter, D (mm)	9.97
Transverse tube pitch, Pt (mm)	31.75
Longitudinal tube pitch, p _l (mm)	17.5
The fin pitch, Fp (mm)	3.21
Fin thickness, Ft (mm)	0.2
Reynolds number, Re	150, 400, 600, 800, 1200
Tube, fin material	Aluminium
Thermal conductivity of fin, k _f (W m ⁻¹ K ⁻¹)	229.111

4. Pressure boundary condition at the outlet border.
5. Symmetry boundary condition on the side surfaces of the computational domain. As this condition is appropriate when the system exhibits symmetry, meaning that the vertical derivative of all variables is zero.
6. Periodic boundary condition on two upper and lower boundaries passing through the middle distance of the fins. This condition suits scenarios where the flow's geometry and physics exhibit repetitive states and similar units.

Conservation of mass equation is expressed as:

$$\vec{\nabla} \cdot \vec{V} = 0 \quad (1)$$

Momentum conservation equations is defined as:

$$\rho(\vec{\nabla} \cdot \vec{V})\vec{V} = -\vec{\nabla}p + \mu\nabla^2\vec{V} \quad (2)$$

Energy conservation is:

$$\rho(\vec{\nabla} \cdot \vec{V})\vec{V} = -\vec{\nabla}p + \mu\nabla^2\vec{V} \quad (3)$$

The friction factor, established by the pressure drop of the finned tube heat exchanger, is:

$$f = \frac{(p_{in}-p)H}{\frac{1}{2}\rho u_{in}^2 4L} \quad (4)$$

The coefficient of heat transfer, predicated upon the logarithmic mean temperature difference and the transfer of heat from tubes and fins to the fluid, is:

$$Q = \dot{m}C_p(T_{in} - T_{out}) = hA\Delta T \quad (5)$$

Logarithmic average temperature difference is expressed as:

$$\Delta T = \frac{(T_w-T_{in})-(T_w-T_{out})}{\ln[(T_w-T_{in})/(T_w-T_{out})]} \quad (6)$$

The Reynolds number, predicated on the inlet velocity and the distance between the fins as described by [Yaïci et al. \(2016\)](#), along with the Nusselt number and Prandtl number, are:

$$Re = \frac{\rho u_{in}H}{\mu} \quad (7)$$

$$Nu = \frac{hH}{k} \quad (8)$$

$$Pr = \frac{C_p\mu}{k} \quad (9)$$

The Colburn factor is:

$$j = \frac{Nu}{RePr^{\frac{1}{3}}} \quad (10)$$

According to [Modi et al. \(2020\)](#), the flow area goodness factor is:

$$\frac{j}{f} = \frac{Nu.pr^{-\frac{1}{3}}}{f.Re} \quad (11)$$

Performance Evaluation Criteria (PEC) assesses the advantages of improved heat transfer performance from the expanded area against the disadvantages of increased pressure drop. This method makes it possible to evaluate heat transfer performance concerning pressure decrease in a balanced manner. The PEC coefficient is presented in

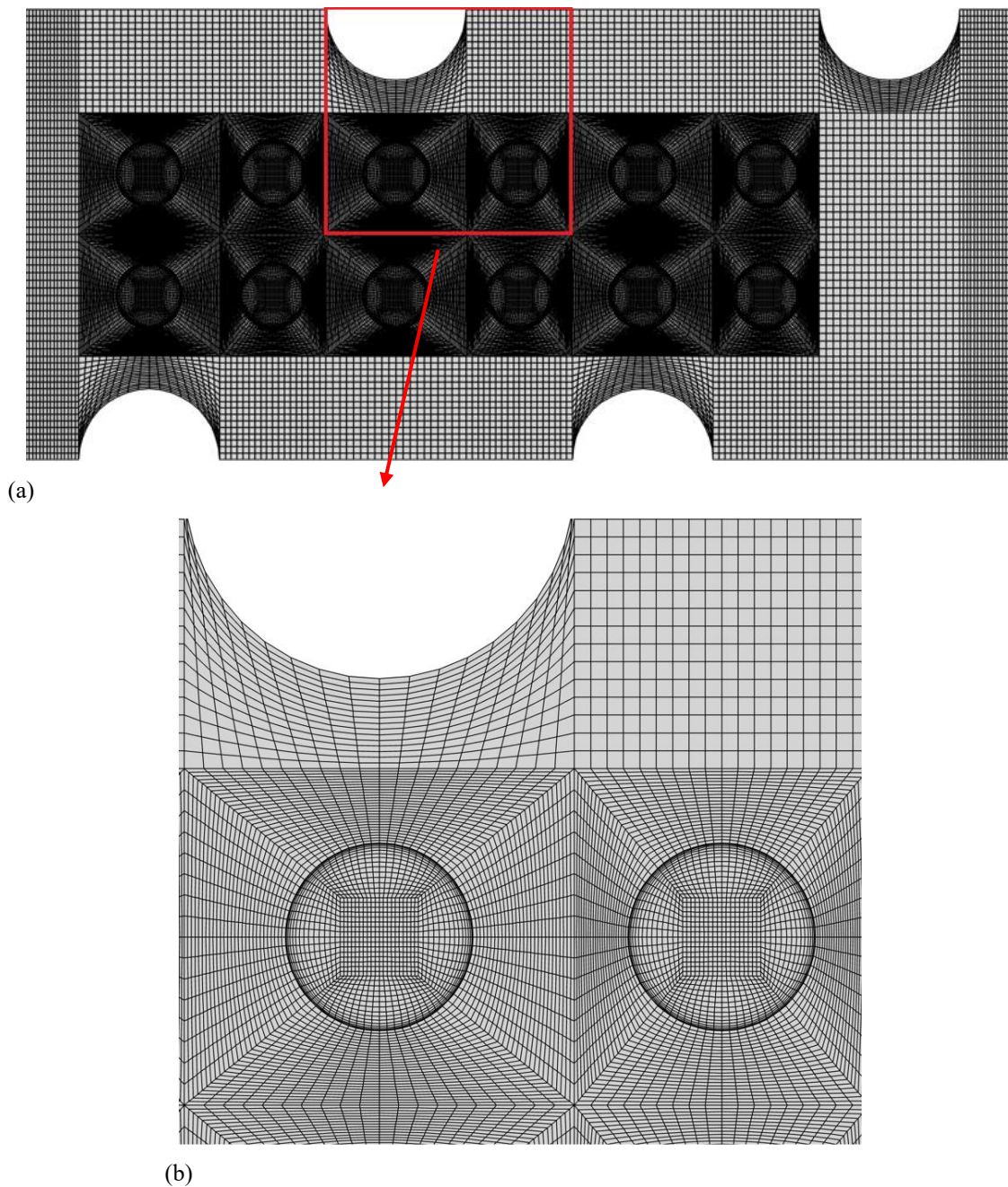


Fig. 3 Computational grid of the finned tube with dimples-protrusions

this investigation to enable a comprehensive evaluation of different dimple configurations and find a compact heat exchanger model that maximizes heat transfer performance while minimizing pressure drop. According to Paul et al. (2023), the equation of PEC is:

$$PEC = \frac{Nu}{Nu_0} / \left(\frac{f}{f_0}\right)^{\frac{1}{3}} \quad (12)$$

Where Nu_0 and f_0 represent the Nusselt number and the friction factor of the plain fin, respectively.

The SIMPLEC algorithm is proposed for addressing the coupling of pressure and velocity, the Standard scheme is employed for discretizing the governing equation of pressure, and the QUICK scheme is for momentum and energy. Also, the residuals of the equations of momentum,

conservation of mass, and energy are set equal to 10^{-6} . In this research, the thermophysical properties of air are considered based on the mean temperature of the inlet and outlet.

4. THE STUDY OF THE NON-DEPENDENCE OF RESULTS ON COMPUTING MESHING

The meshing process is carried out utilizing a quadrilateral model. The general geometry comprises two distinct parts, solid and fluid, with the grid cells being regularly placed atop each other at the interface of these two parts. Moreover, the Hexa method is employed adjacent to the tube border. Figure. 3 illustrates the computational grid. Three different computational cell

Table 2 Grid independence according to the Nusselt number and friction coefficient

Cases	The numbers of computational cells	Nusselt number	Friction factor
1	950000	4.12	0.1221
2	1450000	4.30	0.1289
3	1800000	4.31	0.1291

numbers are studied. The computational cell numbers are 950000, 1450000, and 1800000. Table 2 demonstrates the grid independence of the numerical solutions for model (a) based on the Nusselt number and friction coefficient. The variance in results presented in the number of computational grids in cases 2 and 3 is less than 0.3%. Ultimately, a grid independence examination is performed for all the computational models, and the number 1450000 is selected for both model (a) and model (b). And for model (c), the number 1750000 is chosen.

5. VALIDATION

This research utilizes the experimental study by Wang et al. (1996) and the numerical study by Yaïci et al. (2016) to validate the performance of a finned-tube heat exchanger with plain fins. The following simulation mirrors the characteristics of the studies mentioned above. The number of tube rows is equal to 4, as well as the longitudinal pitch of the tube is 22 mm, the transverse pitch is 25.4 mm, the fin pitch is 3 mm, the fin thickness is 0.13 mm, and the tube's diameter is 9.5 mm. The temperature of the air inlet is 298K, and the wall temperature is 373K. Figure. 4 presents a detailed comparison of the findings from the present study with those published by Wang et al. (1996) and Yaïci et al. (2016) regarding the *j* coefficient and the friction coefficient. The *j* coefficient's relative error lies within the range of 8% to 20%, while the friction coefficient's relative error confines between less than 3% and 13%. The present simulation outcomes are also compared to the numerical findings of Yaïci et al. (2016). The relative error for the *j* coefficient ranges from 4% to 20%, while the relative error for the friction coefficient falls between 12% and 20%.

Figure 5 displays the temperature contour of the fluid at the midplane between two half-fins within the heat exchanger with plain fins. As the boundary layer of thermal initiates in the tubes and fins region, the fluid's temperature gradually rises. Notably, the temperature of the fluid in the primary area is lower than that of the tubes and fins. Therefore, heat is transferred from tubes and fins to the fluid, increasing fluid temperature. Furthermore, given that heat transfer from tubes to fins and fluid occurs, the tubes act as the main source of heat transfer. Consequently, close to the tube surfaces, the fluid temperature increases. Table 3 presents the distribution of heat transfer to the fluid for fins and tubes individually, as well as the proportion of heat transfer to the fluid at a Reynolds number of 150.

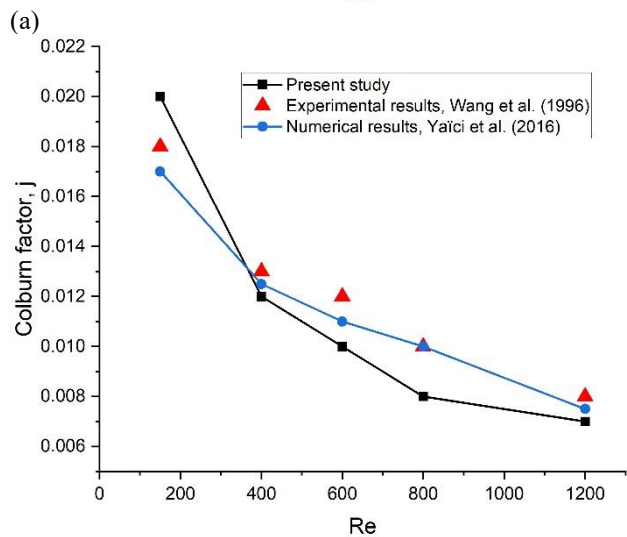
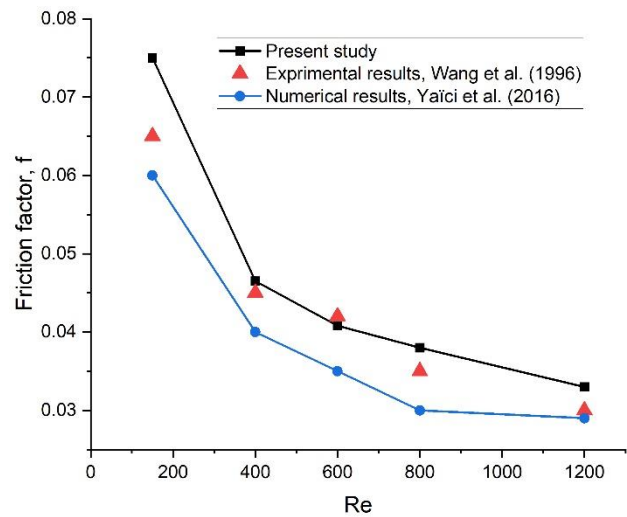


Fig. 4 Evaluation of the present study with the experimental outcomes of Wang et al. (1996) and the numerical study of Yaïci et al. (2016)

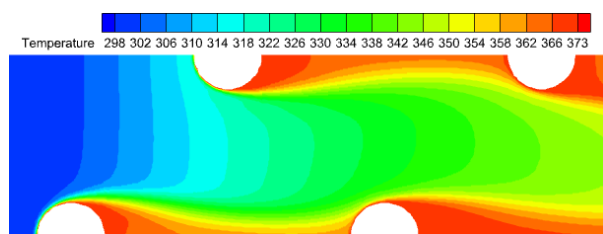


Fig. 5 Contour of fluid temperature at the midplane between two half-fins at Re=150

Table 3 Distribution of heat transfer to fluid at Re=150

Cases	Tube and fin	Q (W)	Heat transfer percentage
a	Tube 1	0.083	1.93
b	Tube 2	0.092	2.15
c	Tube 3	0.022	0.51
d	Tube 4	0.012	0.28
e	Fins	4.081	95.13
f	Total	4.290	100

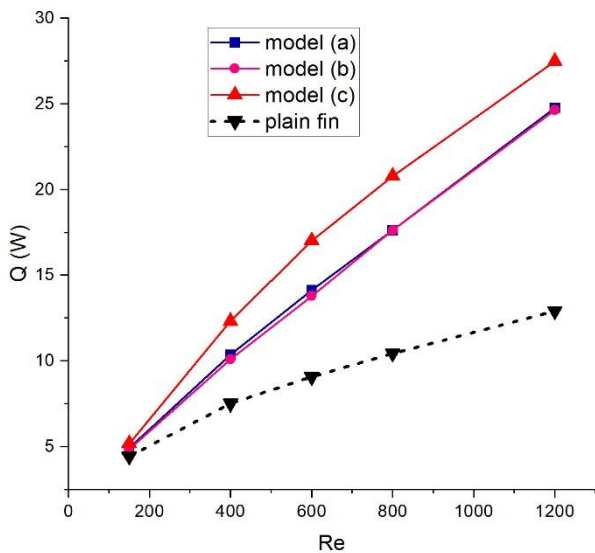


Fig. 6 Outcomes of the heat transfer evaluation performed on the plain fin and its variant featuring dimples and protrusions

6. RESULTS

The findings of Lotfi and Sunden. (2019) revealed that the implementation of dimples led to an augmentation of heat transfer, and the present investigation noted an enhancement in heat transfer in comparison to heat exchangers that possess plain fins. Figure 6 presents the heat transfer results of both plain fins and fins that possess dimples-protrusions for comparative purposes. Upon scrutiny, it is evident that the outcomes of heat transfer for model (a) and (b) are close to each other. Significantly, the most notable increase in heat transfer, in comparison to the plain fin, is 91%. However, it is significant to note that in model (c), there is a substantial difference that can be observed in the heat transfer results in contrast to the other two models. Furthermore, in model (c), there is a considerable increase in heat transfer compared to the plain fin, with the highest difference being 112%, while the lowest increase in heat transfer, in contrast to the plain fin, is 16%. Furthermore, the integration of hemispheres into the fins creates obstructions to the flow, resulting in a significant gain in pressure drop in contrast to the plain fin.

Valentino et al. (2012) executed an investigation utilizing dimples across three distinct geometrical configurations within the heat exchanger, revealing that the main notable enhancement in heat transfer occurred in the model featuring the largest dimple, which registered an increase ranging from 33% to 54%. Conversely, in the present investigation, the observed highest augmentation in heat transfer spans from 16% to 112%. According to the Chilton-Cleburn analogy by Incropera et al. (1996), heat transfer and pressure drop are directly correlated, indicating that an increment in pressure drop corresponds with an increase in heat transfer. Consequently, any factors that induce rotation and deflection of the flow lines result in an enhancement

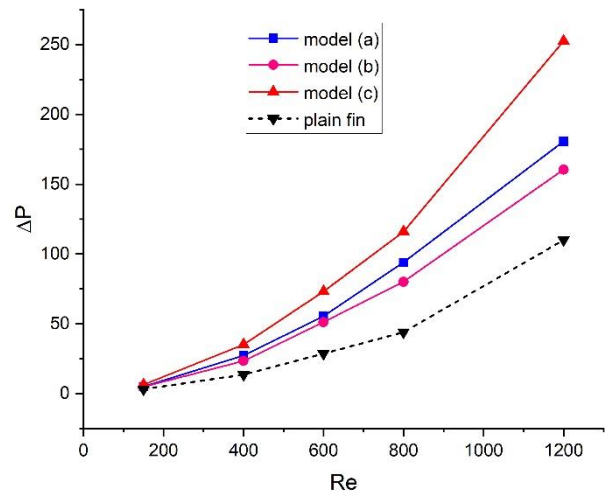


Fig. 7 Comparison of pressure drop in various models relative to plain fin

of the pressure drop, thereby facilitating an augmentation of the heat transfer. Figure 7 indicates the pressure drop in different models. In light of the substantial quantity of protrusions-dimples present in model (c), the rotational of the fluid in this configuration exceeds those observed in other models, resulting in model (c) exhibiting the most significant pressure drop.

Figure 8 (a) depicts the velocity contour at the midplane between two half-fins within the heat exchanger with dimples-protrusions on fins. As the fluid encounters these hemispherical structures, its velocity decreases. Moreover, as we move away from these protrusions in contrast to the transverse pitch, the velocity experiences an enhancement. Figure 8 (b) illustrates the temperature contour of the fluid situated in the middle distance of two half-fins. The plane that passes through the midplane of these two half-fins also intersects the protrusions due to their considerable height. As the thermal boundary layer occurs in the tube-fin region, the fluid temperature begins to escalate. The heat transfer takes place from the tubes and fins to the fluid. Near the tubes, which serve as the primary source of heat transfer, the fluid temperature is the highest. Additionally, behind the protrusions, an increase in the fluid temperature is observed because, at this region, the separation of flow and return flows encountered, resulting in the entrapment of fluid within these regions, impeding its progress with the overall flow and consequently leading to temperature elevation in these specific areas. The augmentation of the output temperature occurs as the result of the expansion of the fin's cross-sectional area facilitated by affixing dimples-protrusions. In Fig 8 (c), similar to the inline configuration, the fluid confronts obstructions along its path, leading to decreased velocity due to the formation of reverse flows. In Fig 8 (d), as the fluid temperature at the outlet significantly influences the improvement of heat transfer, the enhancement in fluid temperature at the outlet within the staggered arrangement model is comparatively lower than that of the inline arrangement model.

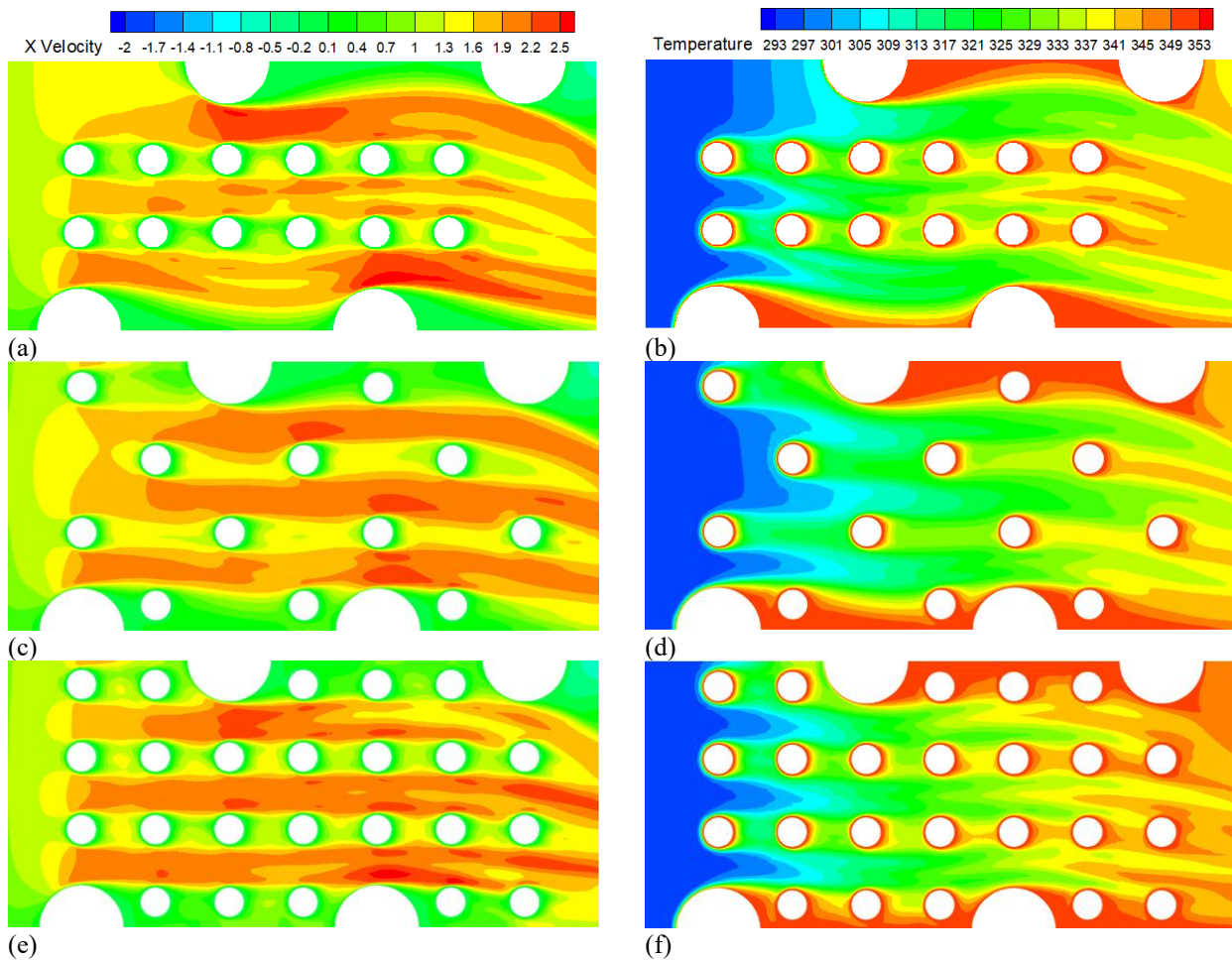


Fig. 8 (a) Contour of horizontal component of velocity, (b) contour of temperature in the middle distance between two half-fins at $Re=150$

In Fig 8 (e), alterations in velocity have been noted at multiple locations within model (c) due to the abundance of impediments present along the flow path. In Fig. 8 (f), because the separation of flow and return flow exist in more places, the temperature has increased in more parts, and the output temperature has increased compared to other models. Due to the inherent asymmetry in the geometric configuration, the contours of velocity and temperature exhibit a downward deviation attributable to the specific arrangement of the staggered tubes, in which the upper and lower tubes do not face each other. Figure. 9 depicts the path lines of fluid flow on the surface of the fin as well as the protrusions. The flow lines encounter hemispherical obstacles and subsequently traverse over the protrusions. Moreover, the presence of reverse flow can be observed behind these protrusions.

According to the investigation conducted by Lotfi and Sunden. (2019) utilized leeward triangular dimple, Fan et al. (2012) employed elliptical dimples in a finned-tube heat exchanger, while Wu et al. (2014) operated hemispherical dimples. All three studies observed an increase in the Nusselt number in contrast to a plain fin. In comparison to the previous data, the present investigation yielded more enhancement in the Nusselt number. The difference between the maximum enhancement in the Nusselt number in the present study

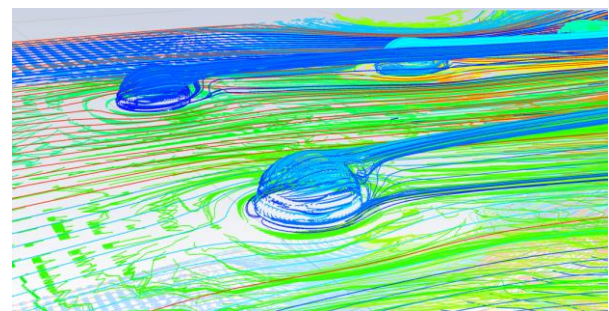
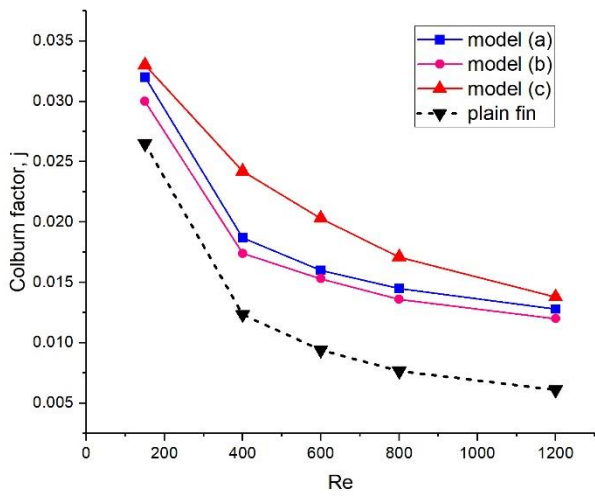
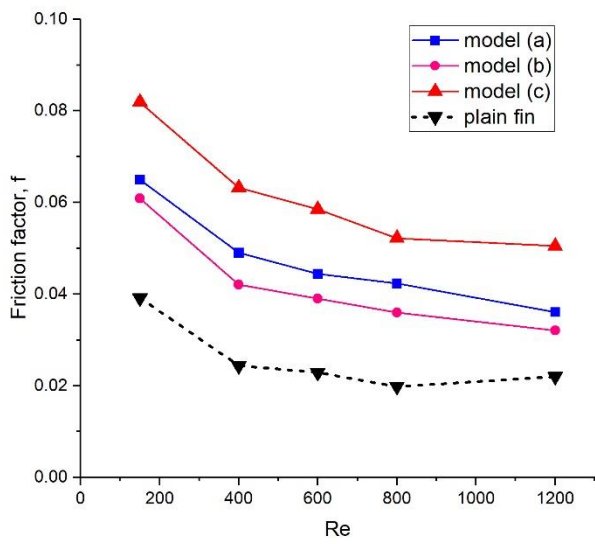


Fig. 9 Path lines on the surface of the lower fin along with the protrusions

and mentioned studies of Lotfi and Sunden. (2019), Fan et al. (2012), and Wu et al. (2014) are 70%, 92%, and 46%, respectively. For fins with dimples-protrusions, the heat flux entering the fluid from the tubes and the fins increases, thereby augmenting the Nusselt number and, consequently, the j coefficient compared to the plain fin. In model (a), the maximum percentage increase of the j coefficient at the Reynolds number of 1200 is 110%, and the friction coefficient at the Reynolds number of 800 is 113%. The minimum percentage increase of the j coefficient at the Reynolds number of 150 is 21%, and the friction coefficient at the Reynolds number of 1200 is 64%.



(a)



(b)

Fig. 10 Comparing the j coefficient, and friction coefficient of the heat exchanger with plain fins and fins with dimples-protrusions

In an examination of the impact of the dimples-protrusions arrangement, it is found that the inline arrangement exhibits a higher j coefficient than the staggered arrangement, albeit with a slight difference percentage. Additionally, the inline arrangement demonstrates a higher friction coefficient than the staggered arrangement. With regards to model (c), which serves as an investigation into the effect of the number of dimples-protrusions on the results, the highest increase of the j coefficient compared to the plain fin is 127%, whereas the lowest increase is 25%. Upon increasing the number of dimples-protrusions, which function as additional obstacles in the trajectory of the flow, the pressure drop significantly increases, leading to a corresponding enhancement in the friction coefficient.

In light of this explanation, the most enhancement in the friction coefficient in model (c) compared to the plain fin is 163%, whereas the lowest increase is 108%. Upon conducting an analysis, the number of dimples-protrusions in model (c) exhibits significantly higher values for heat transfer, j coefficient, and friction

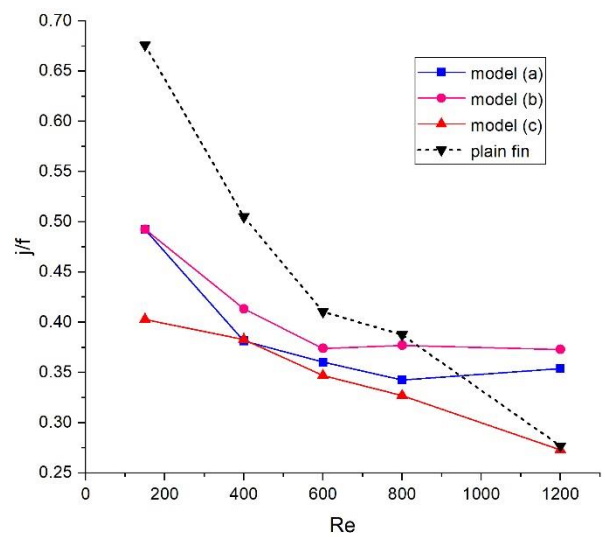


Fig. 11 Comparison of flow area goodness factor

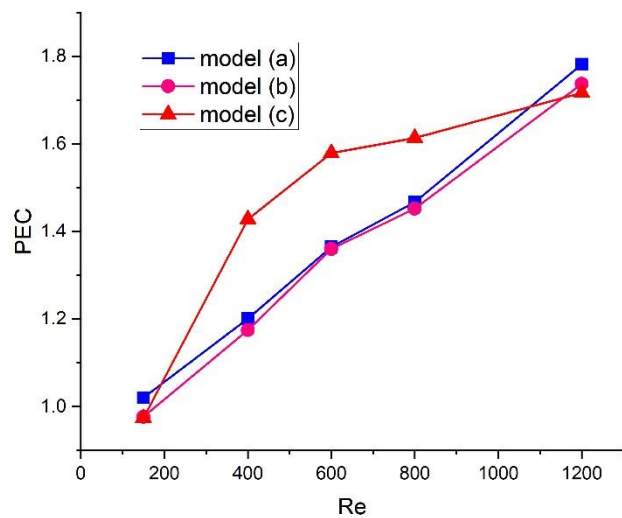


Fig. 12 Comparison of PEC values

coefficient in comparison to the findings of model (a) and (b). In Fig. 10, the outcomes of the j coefficient and the friction coefficient are presented for the heat exchanger equipped with plain fins and with dimples-protrusions. Through this study, it is determined that an enhancement in the Reynolds number causes a decline in both the j coefficient and the friction coefficient. Figure 11 shows flow area goodness factor ($\frac{j}{f}$) in different Reynolds number, this ratio is introduced to examine the design of the heat exchanger in new geometric using dimples. Figure 12 presents the PEC values for three models that optimize the finned-tube heat exchanger with dimples and protrusions. The first and second models exhibit nearly identical PEC values. In the first model, the PEC values exceed 1 for all Reynolds numbers, peaking at 1.782 when the Reynolds number is 1200.

7. CONCLUSIONS

In the examination of the impact of dimples-protrusions on the finned-tube heat exchanger for pressure drop and heat transfer at varying Reynolds numbers, the

heat transfer demonstrates an increment in comparison to the plain fin. Additionally, owing to the existence of obstacles in the flow path, an upsurge in pressure drop is inevitable. The key conclusions from the investigation are:

1. The augmentation of dimples-protrusions quantity has a substantial effect on the j coefficient value, as it enhances the coefficient of heat transfer, leading to an escalation in the Nusselt number and ultimately, elevating the j coefficient in comparison to other models.
2. Model (c), due to its extensive quantity of dimples-protrusions, amplifies the fluid outlet temperature, ultimately resulting in the highest heat transfer in model (c) compared to other models.
3. The outcomes of heat transfer and the results of the j coefficient in both staggered and inline arrangements are close. It is also noteworthy that the friction coefficient of model (a) surpasses that of model (b).
4. As the hemispheres pose barriers to the flow, a rise in the quantity of dimples-protrusions leads to a significant enhancement in the friction coefficient in this particular model compared to other models.

CONFLICT OF INTEREST

There are no pertinent financial or non-financial conflicts of interest to disclose.

AUTHOR CONTRIBUTIONS

Omid Baharlouei performed computations and carried out the numerical analysis. **Omid Baharlouei** and **Shahram Talebi** deliberated on the findings and participated in the completion of the ultimate manuscript. **Shahram Talebi** supervised the outcomes of this study.

REFERENCES

- Aroonrat, K., & Wongwiset, S. (2019) Experimental investigation of condensation heat transfer and pressure drop of R-134a flowing inside dimpled tubes with different dimpled depths. *International Journal of Heat and Mass Transfer*, 128, 783-793. <https://doi.org/10.1016/j.ijheatmasstransfer.2018.09.039>
- Azad, G. S., Huang, Y., & Han, J. (2000). Impingement heat transfer on dimpled surfaces using a transient liquid crystal technique. *Journal of thermophysics and heat transfer*, 14(2), 186-193. <https://doi.org/10.2514/2.6530>
- Bi, C., Tang, G., & Tao, W. (2013). Heat transfer enhancement in mini-channel heat sinks with dimples and cylindrical grooves. *Applied Thermal Engineering* 55(1-2), 121-132. <https://doi.org/10.1016/j.applthermaleng.2013.03.007>
- Cheraghi, M. H., Ameri, M., & Shahabadi, M. (2020). Numerical study on the heat transfer enhancement and pressure drop inside deep dimpled tubes. *International Journal of Heat and Mass Transfer* 147, 118845. <https://doi.org/10.1016/j.ijheatmasstransfer.2019.118845>
- Du, W., Luo, L., Wang, S., & Zheng, X. (2020). Heat Transfer Characteristics in a Pin Finned Channel With Different Dimple Locations. *Heat Transfer Engineering* 41(14), 1232-1251. <https://doi.org/10.1080/01457632.2019.1637114>
- Elsaid, A. M., Abdelhady, A. M., Abdelaziz, G. B., & Halim, M. A. (2023). Performance improvement for chilled water air conditioning cooling coils with various dimple fin geometries. *International Journal of Thermal Sciences*, 193, 108441. <https://doi.org/10.1016/j.ijthermalsci.2023.108441>
- Fan, J. F., Ding, W. K., He, Y. L., & Tao, W. Q. (2012). Three-dimensional numerical study of fluid and heat transfer characteristics of dimpled fin surfaces. *Numerical Heat Transfer; Part A: Applications*, 62(4), 271-294. <https://doi.org/10.1080/10407782.2012.666931>
- Gupta, A., Kumar, M., & Patil, A. K., (2019) Enhanced heat transfer in plate fin heat sink with dimples and protrusions. *Heat and Mass Transfer*, 55(8), 2247-2260. <https://doi.org/10.1007/s00231-019-02561-w>
- Hwang, S., Kim, D., Min, J., & Jeong, J. (2012). CFD analysis of fin tube heat exchanger with a pair of delta winglet vortex generators. *Journal of Mechanical Science and Technology*, 26(9), 2949-2958. <https://doi.org/10.1007/s12206-012-0702-2>
- Incropera, F. P., DeWitt, D. P., Bergman, T. L., & Lavine, A. S. (1996). *Fundamentals of heat and mass transfer* (6, 116). Wiley.
- Jing, Q., Xie, Y., & Zhang, D. (2019). Effects of channel outlet configuration and dimple/protrusion arrangement on the blade trailing edge cooling performance. *Applied Sciences*, 9(14), 2900. <https://doi.org/10.3390/app9142900>
- Kaood, A., Aboulmagd, A., Othman, H., & ElDegwy, A. (2022). Numerical investigation of the thermal-hydraulic characteristics of turbulent flow in conical tubes with dimples. *Case Studies in Thermal Engineering*, 36, 102166. <https://doi.org/10.1016/j.csite.2022.102166>
- Katkhaw, N., Vorayos, N., Kiatsiriroat, T., Khunatorn, Y., Bunturat, D., & Nuntaphan, A. (2014). Heat transfer behavior of flat plate having 45 ellipsoidal dimpled surfaces. *Case Studies in Thermal Engineering* 2, 67-74. <https://doi.org/10.1016/j.csite.2013.12.002>
- Kumar, A., Maithani, R., Raj, A., & Suri, S. (2017). Numerical and experimental investigation of enhancement of heat transfer in dimpled rib heat exchanger tube. *Heat and Mass Transfer*, 53, 3501-3516. <https://doi.org/10.1007/s00231-017-2080-x>
- Li, M., Khan, T. S., Al-hajri, E., & Ayub, Z. H. (2016). Single phase heat transfer and pressure drop analysis of a dimpled enhanced tube. *Applied Thermal Engineering* 101, 38-46.

- <https://doi.org/10.1016/j.applthermaleng.2016.03.042>
- Lotfi, B., & Sunden, B. (2019). Thermo-hydraulic performance enhancement of finned elliptical tube heat exchangers by utilizing innovative dimple turbulators. *Heat Transfer Engineering*, 41(13), 1117-1142. <https://doi.org/10.1080/01457632.2019.1611132>
- Luo, D., Li, Z., Yan, Y., Yang, L., Cao, J., Yang, X., & Cao, B. (2024). Design and optimization of a thermoelectric generator with dimple fins to achieve higher net power. *Applied Thermal Engineering*, 123735. <https://doi.org/10.1016/j.applthermaleng.2024.123735>
- Luo, L., Wang, C., Wang, L., Sunden, B., & Wang, S. (2016). Heat transfer and friction factor performance in a pin fin wedge duct with different dimple arrangements. *Numerical Heat Transfer; Part A: Applications*, 69(2), 209–226. <https://doi.org/10.1080/10407782.2015.1052301>
- Malapur, H. V., Havaldar, S. N., & Kharade, U. V. (2022). Heat transfer enhancement of an internally and externally dimpled pipe heat exchanger–Numerical study. *Materials Today: Proceedings*, 63, 587-594. <https://doi.org/10.1016/j.matpr.2022.04.155>
- Mehrijardi, S. A. A., Khademi, A., Said, Z., Ushak, S., & Chamkha, A. J. (2023). Effect of elliptical dimples on heat transfer performance in a shell and tube heat exchanger. *Heat and Mass Transfer*, 59(10), 1781-1791. <https://doi.org/10.1007/s00231-023-03367-7>
- Modi, A., Kalel, N., & Rathod, M. (2020). Thermal performance augmentation of fin-and-tube heat exchanger using rectangular winglet vortex generators having circular punched holes. *International Journal of Heat and Mass Transfer*, 158, 119727. <https://doi.org/10.1016/j.ijheatmasstransfer.2020.119724>
- Paul, S., Lubaba, N., Pratik, N. A., Ali, M. H., & Alam, M. M. (2023). Computational investigation of cross flow heat exchanger: A study for performance enhancement using spherical dimples on fin surface. *International Journal of Thermofluids*, 20, 100483. <https://doi.org/10.1016/j.ijft.2023.100483>
- Piper, M., Zibart, A., Djakow, E., Springer, R., Homberg, W., & Kenig, E. Y. (2019). Heat transfer enhancement in pillow-plate heat exchangers with dimpled surfaces: A numerical study. *Applied Thermal Engineering*, 153, 142-146. <https://doi.org/10.1016/j.applthermaleng.2019.02.082>
- Rao, Y., Li, B., & Feng, Y. (2015). Heat transfer of turbulent flow over surfaces with spherical dimples and teardrop dimples. *Experimental Thermal and Fluid Science*, 61, 201–209. <https://doi.org/10.1016/j.expthermflusci.2014.10.030>
- Rao, Y., Wan, C., & Xu, Y. (2012a). An experimental study of pressure loss and heat transfer in the pin fin-dimple channels with various dimple depths. *International Journal of Heat and Mass Transfer*, 55(23–24), 6723–6733. <https://doi.org/10.1016/j.ijheatmasstransfer.2012.06.081>
- Rao, Y., Xu, Y., & Wan, C. (2012b). An experimental and numerical study of flow and heat transfer in channels with pin fin-dimple and pin fin arrays. *Experimental Thermal and Fluid Science* 38, 237-247. <https://doi.org/10.1016/j.expthermflusci.2011.12.012>
- Sangtarash, F., & Shokuhmand, H. (2015). Experimental and numerical investigation of the heat transfer augmentation and pressure drop in simple, dimple and perforated dimple louver fin banks with an inline or staggered arrangement. *Applied Thermal Engineering* 82, 194-205. <https://doi.org/10.1016/j.applthermaleng.2015.02.073>
- Seo, Y., Lee, H., Jeon, S., Ku, T., Kang, B., & Kim, J. (2012). Homogenization of Dimpled Tube and Its Application to Structural Integrity Evaluation for a Dimple-type EGR Cooler using FEM. *International Journal of Precision Engineering and Manufacturing*, 13(2), 183–191. <https://doi.org/10.1007/s12541-012-0023-5>
- Sen, P., Chen, M., & Bai, B. (2024). Heat transfer enhancement of air flow through new types of perforated dimple/protrusion fins. *Applied Thermal Engineering*, 256, 124030. <https://doi.org/10.1016/j.applthermaleng.2024.124030>
- Song, K., Yang, Q., Sun, K., Wu, X., Zhang, Q., & Hou, Q. (2024). Performance promotion by novel fin configurations with ellipsoidal dimple-protrusion for a circle tube-fin heat exchanger. *International Communications in Heat and Mass Transfer*, 157, 107731. <https://doi.org/10.1016/j.icheatmasstransfer.2024.107731>
- Valentino, M., Tran, L., Ricklick, M., & Kapat, J. (2012). A study of heat transfer augmentation for recuperative heat exchangers: Comparison between three dimple geometries. *Journal of Engineering for Gas Turbines and Power* 134(7). <https://doi.org/10.1115/1.4005990>
- Vignesh, S., Moorthy, V. S., & Nallakumarasamy, G. (2017). Experimental and CFD analysis of concentric dimple tube heat exchanger. *International Journal of Emerging Technologies in Engineering Research (IJETER)*, 5(7), 18–26.
- Vorayos, N., Katkhaw, N., Kiatsiriroat, T., & Nuntaphan, A. (2016). Heat transfer behavior of flat plate having spherical dimpled surfaces. *Case Studies in Thermal Engineering*, 8, 370–377. <https://doi.org/10.1016/j.csite.2016.09.004>
- Wang, C., Chang, Y. J., Hsieh, Y. C., Lin, Y. T. (1996) Sensible heat and friction characteristics of plate fin-and-tube heat exchangers having plane fins.

- International Journal of Refrigeration*, 19(4), 223–230. [https://doi.org/10.1016/0140-7007\(96\)00021-7](https://doi.org/10.1016/0140-7007(96)00021-7)
- Wang, Y., Li, S., Xie, X., Deng, Y., Liu, X., & Su, C. (2018). Performance evaluation of an automotive thermoelectric generator with inserted fins or dimpled-surface hot heat exchanger. *Applied Energy*, 218, 391–401. <https://doi.org/10.1016/j.apenergy.2018.02.176>
- Wang, Y., Li, S., Yang, X., Deng, Y., & Su, C. (2016). Numerical and experimental investigation for heat transfer enhancement by dimpled surface heat exchanger in thermoelectric generator. *Journal of Electronic Materials*, 45(3), 1792–1802. <https://doi.org/10.1007/s11664-015-4228-0>
- Wu, X., Feng, L., Liu, D., Meng, H., & Lu, Y. (2014). Numerical study on the effect of tube rows on the heat transfer characteristic of dimpled fin. *Advances in Mechanical Engineering*, 6, 637052. <https://doi.org/10.1155/2014/637052>
- Xie, S., Liang, Z., Zhang, L., Wang, Y., Ding, H., & Zhang, J. (2018). Numerical investigation on heat transfer performance and flow characteristics in enhanced tube with dimples and protrusions. *International Journal of Heat and Mass Transfer*, 122, 602-613. <https://doi.org/10.1016/j.ijheatmasstransfer.2018.01.106>
- Yaïci, W., Ghorab, M., & Entchev, E. (2016). 3D CFD study of the effect of inlet air flow maldistribution on plate-fin-tube heat exchanger design and thermal-hydraulic performance. *International Journal of Heat and Mass Transfer*, 101, 527-541. <https://doi.org/10.1016/j.ijheatmasstransfer.2016.05.063>
- Ying, P., He, Y., Tang, H., & Ren, Y. (2021). Numerical and experimental investigation of flow and heat transfer in heat exchanger channels with different dimples geometries. *Machines*, 9(4), 72. <https://doi.org/10.3390/machines9040072>
- Zheng, F. C., Liu, Z., Lin, M., Nugud, J., Wang, L. C., Chang, L. M., & Wang, L. B. (2018). Experimental study on heat transfer performances of flat tube bank fin heat exchanger using four different fin patterns. *Journal of Heat Transfer*, 140(4). <https://doi.org/10.1115/1.4038419>